Numerical Analysis and Design Optimisation of Leaf Spring Using SolidWorks 2020 & ANSYS 18.1

Abhishek Gautam[1] Dr. Rajesh Kumar Satankar[2]
[1]PG Scholar [2]Associate Professor
[1,2]Department of Mechanical Engineering
[1,2]Jabalpur Engineering College, Jabalpur, India

Abstract — This study article describes the many kinds of content. and discover the ideal leaf spring This research presents a comprehensive analysis and design process for leaf springs using SolidWorks and ANSYS, two powerful engineering software tools. Leaf springs are essential components in vehicular suspension systems, providing support and stability for various transportation applications. This study aims to enhance the performance and reliability of leaf springs through a systematic approach that combines 3D modeling, simulation, and optimization techniques and finds more effective and high strength. With many superior qualities, including cost, cost-effectiveness, and weight. With the use of SOLIDWORK2020 & ANSYS18.1, the major goal of this study work is to determine whether the novel radius for leaf springs is more cost-effective and lighter than existing materials.

Keywords: Leaf Spring, Radius, Load, Suspension System Solidwork2020 & Ansys18.1

I. INTRODUCTION

A suspension system consists of a spring and a damper. The energy of road shock causes the spring to oscillate. These oscillations are restricted to a reasonable level by the damper, which is more commonly called a shock absorber. A spring is defined as an elastic body, whose function is to distort when loaded and to recover its original shape when the load is removed.

The leaf spring is main element of the suspension system. It can control for the wheels during acceleration, braking and turning, and general movement caused by the road undulations.

Leaf spring was first introduced in the seventeenth century to support the body of hours drawn coaches. Today, leaf springs are manufactured from carbon steel alloys (low, medium to high alloy), which it has very high yield strength, allowing the spring to return to its original shape after it has been deflected without deformation. Leaf spring leaves are short peened in manufacturing to reduce surface stress and lessen the possibility of a stress riser that could lead to cracked or broken spring.

The stain energy absorbed by the leaf spring needs to be maximized.

The strain energy follows the equation below:

$$u = \sigma^2/2\rho E \quad (1)$$

where:
U = Strain energy,
σ = Strength,
ρ = Density
E = Leaf spring's Young's modulus.

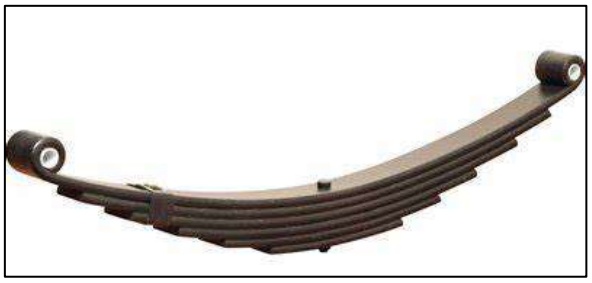

Fig. 1: Leaf spring

II. METHODOLOGY

Here is the process flow diagram to understand the procedure to get results of static structural analysis on leaf spring

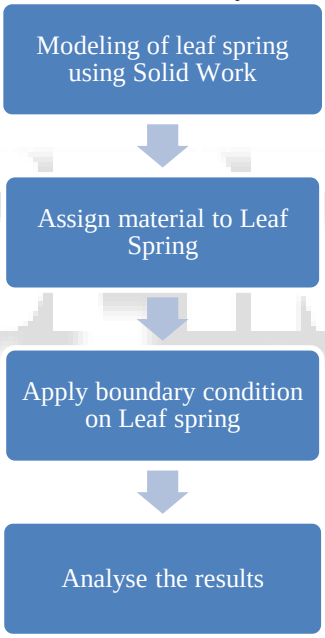

Fig. 2: Flow chart

III. MATERIAL

The term "composite" refers to a structural component that combines two or more materials. The use of composite materials is generally permitted when desired qualities can be obtained. When the constituent elements are employed separately, these desired qualities cannot be obtained. The most prevalent type of composite material is a fibrous composite, which is formed of reinforcing fibres enmeshed in a matrix material.

Acrylic E-glass the term "UD" describes a unidirectional (UD) composite material consisting of E-glass fibres and epoxy resin. By arranging all fibres in a single direction, unidirectional composites are created. Glass-based e-glass fibres possess exceptional levels of strength, stiffness, and chemical resistance. Epoxy resins are thermosetting

polymers with strong chemical resistance, great mechanical qualities, and outstanding adherence to a variety of substrates. Numerous industries, including aerospace, automotive, marine, and sporting goods, employ epoxy E-glass UD. It is employed in the production of structural elements including shells, plates, and beams.

Sr. No.	Parameter	Value
1	Tensile Strength (MPa)	900
2	Compressive Strength (MPa)	450
3	Poisson's Ratio	0.217
4	Density (Kg/m^3)	2.16*10^5
5	Flexural modulus (E) (MPa)	40000

Table 1: Properties of E-Glass/ Epoxy composite leaf spring

IV. MODELING OF LEAF SPRING

Initially the leaf spring has to be designed in the SolidWorks2020 software as a 3D model. The type of spring we designed here is a general shape of multi-leaf spring. Fig.1 which have three levels. With four leaves, from leaf 1 to leaf 4, the first stage is dubbed "make master leaf second stage," and the second stage, known as "helper spring. Third stage create nuts and bolts; fourth stage: assemble all components. This model's distinctive feature is a multi-leaf spring with variable or progressive rate, allowing the ride characteristics to be adjusted across a wide load range. Once the software's designing step is complete, we must use ANSYS software to process the analysis. The SolidWorks file must be saved as a STEP (Standard for the Exchange of Product) file in order to be converted to ANSYS.Figure.2 displays the model created using 3D modeling software.

Fig. 3: 3D model of Leaf Spring

V. THEORETICAL FORMULATION

In this study, the leaf spring has been considered as a single cantilever solid triangle which is an equivalent beam of uniform strength having four-leaf springs for multi-leaf spring, and spring with four leaves of the rectangular cross-section is considered.

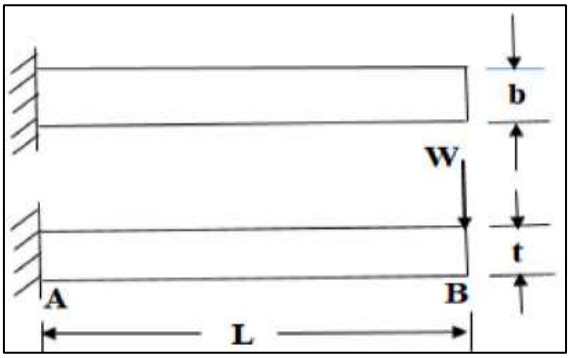

Fig. 4: Leaf spring (cantilever type).

The cantilever beam is extremely visible to both bending and diagonal shear stress. So, the mathematical modeling can be resulting standing from the cantilever sunbeam nature containing a width (b) thickness (t), and length of the plate (L) as shown in Fig. 3. Bending stress in such spring and the maximum deflection for a cantilever with a concentrated load at the free end is given respectively as shown below:

$$\sigma = \frac{M}{Z} = \frac{WL}{\frac{bt^2}{6}} = \frac{6WL}{bt^2} \quad (2)$$

$$\delta_{MAX} = \frac{WL^3}{3EI} = \frac{WL^3}{3E \times \frac{bt^3}{12}} \frac{4WL^3}{Ebt^3} = \frac{2\sigma L^2}{3Et} \quad (3)$$

VI. VALIDATION

The convergence and validation test has been conducted to check the accuracy of the proposed model.

Combined Data of Base paper Validation

Sr. No.	Time Duration	Present work	P.R and K. K
1	0.25	1.4111	1.3111
2	0.50	2.911	2.811
3	0.75	4.1284	4.2284
4	1	5.344	5.2444

Table 2: Deformation(mm)

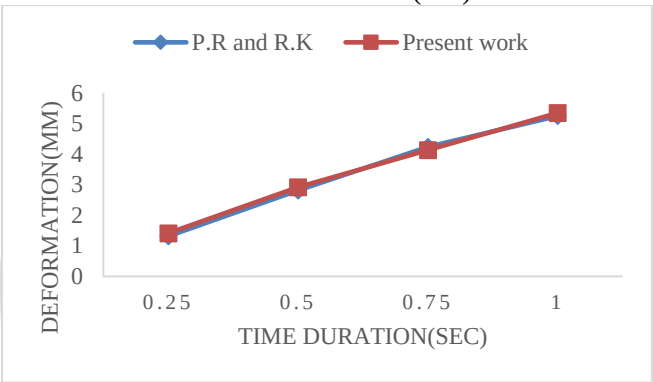

Fig. 5: Comparison Deformation previous and present work

Sr. No.	Time Duration	Present work	P.R and K. K
1	0.25	0.0019466	6.70E-07
2	0.50	0.0038881	0.0028881
3	0.75	0.0058297	0.0048297
4	1	8.99E-03	8.99E-03

Table 3: Strain

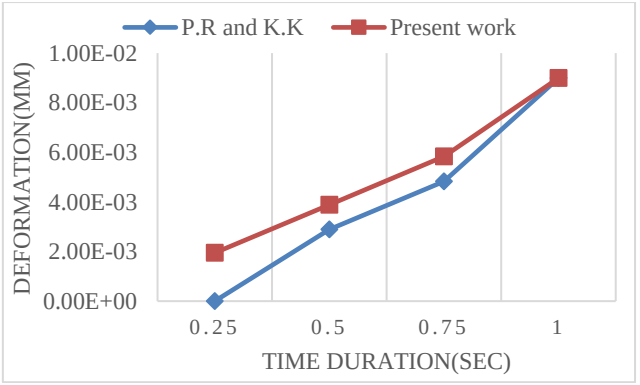

Fig. 6: Comparison Strain previous and present work

Sr. No.	Time Duration	Present work	P.R and K. K
1	0.25	11.957	1.17E+01
2	0.50	23.9	23.3392
3	0.75	35.843	35.0088
4	1	59.11	5.83E+01

Table 4: Stress (Mpa)

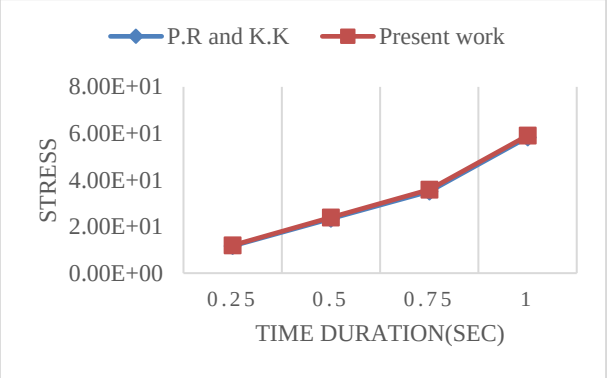

Fig. 7: Comparison Stress previous and present work

VII. RESULTS

The results we obtained from the ANSYS are Total deformation, Equivalent elastic strain, Equivalent Stress (von Mises). All three results are obtained for each radius and each load chosen and compared

After applying a load of 600N, it can be inferred from Fig. 8 the maximum deformation occurred at the 2nd eye which is equal to 6.8735mm. The minimum deformation occurs at the 1st eye which is equal to 0.66135mm Fig.9 denotes the equivalent elastic strain which is minimum at nearby top of the 1st leaf which is equal to 1.2318e-7 unit. Fig.10 shows the maximum stress as 37.712 MPa. The combined data of R1(1150) is given in Table.5

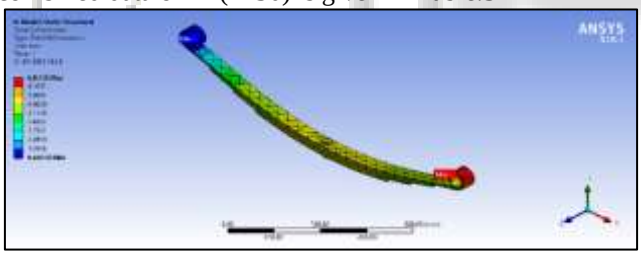

Fig. 8: Analysis image for parameters of R1(1150) Deformation.

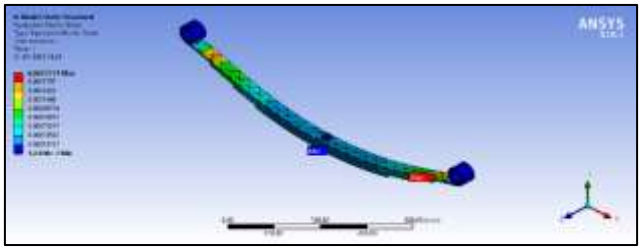

Fig. 9: Analysis image for parameters of R1(1150) Equivalent Elastic Strain.

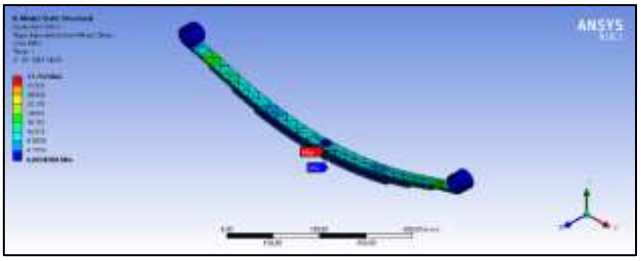

Fig. 10: Analysis image for parameters of R1(1150). Equivalent Stress.

Sr.No.	Parameter	Minimum	Maximum
1	Deformation (mm)	0.66135	6.8735
2	Equivalent elastic strain	1.2318e-7	0.0017771
3	Equivalent stress (Mpa)	0.0018396	37.712

Table 5: Combined Data of R1(1150) and Load 600N

After applying a load of 600 N, it can be inferred from Fig.11, the maximum deformation occurred at the 2nd eye which is equal to 6.1762mm. The minimum deformation occurs at the 1st eye which is equal to 0.62066mm Fig.12, which denotes the equivalent elastic strain which is minimum at near the Centre which is equal to 1.8799e-7 unit. Fig.13, shows the maximum stress as 37.723Mpa. The combined data of R2(1250) is given in Table 6.

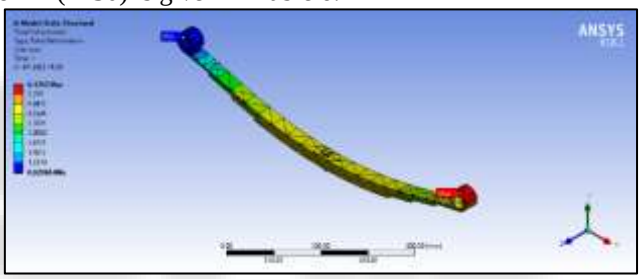

Fig. 11: Analysis image for parameters of R1(1250) Deformation

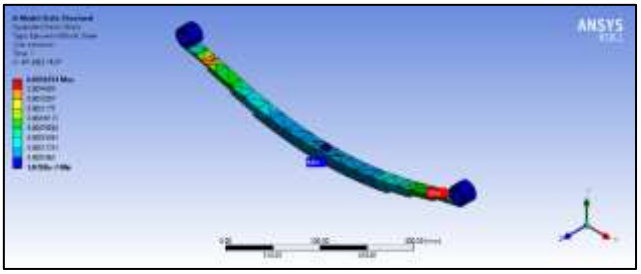

Fig. 12: Analysis image for parameters of R1(1250) Equivalent Elastic Strain.

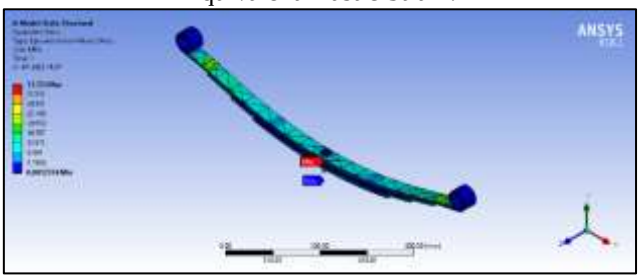

Fig. 13: Analysis image for parameters of R1(1250). Equivalent Stress.

Sr.No.	Parameter	Minimum	Maximum
1	Deformation (mm)	0.62066	6.1762
2	Equivalent elastic strain	1.8799e-7	0.0016761
3	Equivalent stress (Mpa)	0.0012374	37.723

Table 6: Combined Data of R1(1250) and Load 600N

After applying a load of 600 N, it can be inferred from Fig.14, the maximum deformation occurred at the 2nd eye which is equal to 5.4722mm. The minimum deformation occurs at the 1st eye which is equal to 0.60263mm Fig.15, which denotes the equivalent elastic strain which is minimum at near the Centre which is equal to 2.4191e-7 unit. Fig.16, shows the maximum stress as 44.584 Mpa. The combined data of R3(1350) is given in Table 7.

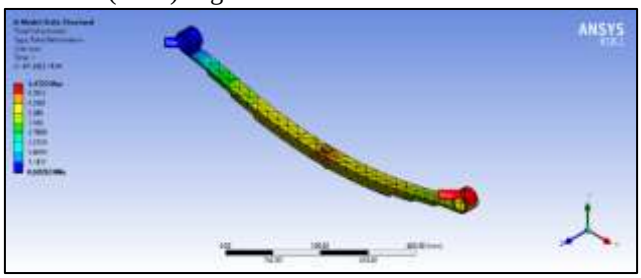

Fig. 14: Analysis image for parameters of R1(1350) Deformation

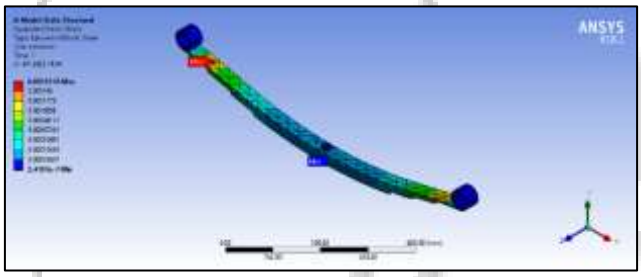

Fig. 15: Analysis image for parameters of R1(1350) Equivalent Elastic Strain.

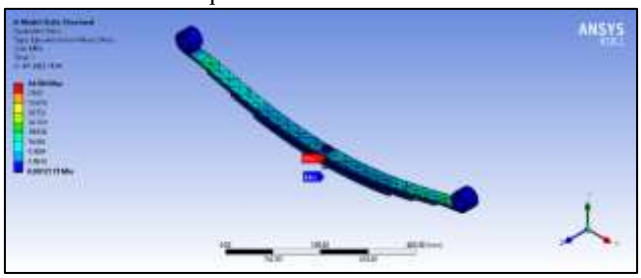

Fig. 16: Analysis image for parameters of R1(1350). Equivalent Stress

Sr.No.	Parameter	Minimum	Maximum
1	Deformation (mm)	0.60263	5.4722
2	Equivalent elastic strain	1e-7	0.0017771
3	Equivalent stress (Mpa)	0.0018396	37.712

Table 7: Combined Data of R1(1350) and Load 600N

After applying a load of 800N, it can be inferred from Fig.17 the maximum deformation occurred at the 2nd eye which is equal to 9.1647 mm. The minimum deformation occurs at the 1st eye Fig.18, denotes the equivalent elastic strain which is minimum at nearby top of the 1st leaf which is equal to 1.6425e-7 unit. Fig. 19, shows the maximum stress as 50.283 MPa. The combined data of R1(1150) is given in Table.8

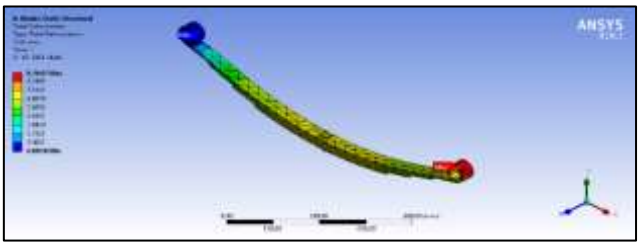

Fig. 17: Analysis image for parameters of R1(1150) Deformation.

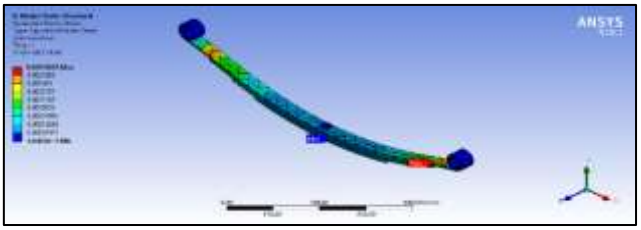

Fig. 18: Analysis image for parameters of R1(1150) Equivalent Elastic Strain.

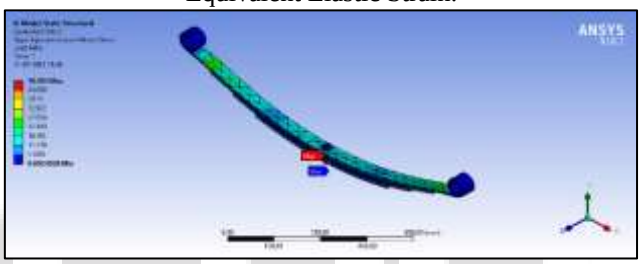

Fig. 19: Analysis image for parameters of R1(1150) Equivalent Stress.

Sr.No.	Parameter	Minimum	Maximum
1	Deformation (mm)	0.8818	9.1647
2	Equivalent elastic strain	1.6425e-7	0.0023695
3	Equivalent stress (Mpa)	0.002458	50.283

Table 8: Combined Data of R1(1150) and Load 800N

After applying a load of 800 N, it can be inferred from Fig.20, the maximum deformation occurred at the 2nd eye which is equal to 8.235 mm. The minimum deformation occurs at the 1st eye. Fig.21, denotes the equivalent elastic strain which is minimum at near the Centre which is equal to 2.506e-7 unit. Fig.22, shows the maximum stress as 50.298 Mpa. The combined data of R2(1250) is given in Table.9.

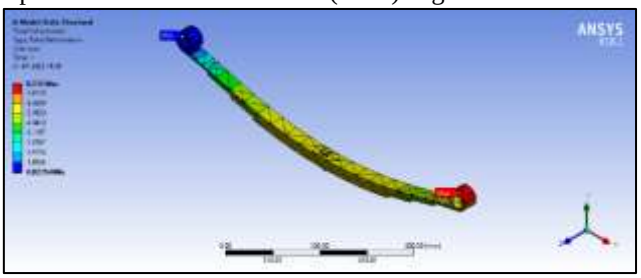

Fig. 20: Analysis image for parameters of R2(1250) Deformation.

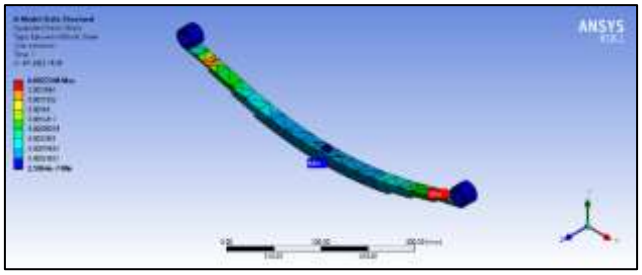

Fig. 21: Analysis image for parameters of R2(1250) Equivalent Elastic Strain.

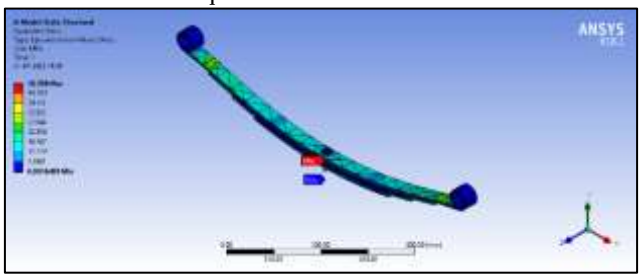

Fig. 22: Analysis image for parameters of R2(1250) Equivalent Stress.

Sr.No.	Parameter	Minimum	Maximum
1	Deformation (mm)	0.82754	8.235
2	Equivalent elastic strain	2.506e-7	0.0022348
3	Equivalent stress (Mpa)	0.0016499	80.298

Table 9: Combined Data of R2(1250)

After applying a load of 800 N, it can be inferred from Fig.23, the maximum deformation occurred at the 2nd eye which is equal to 7.2963 mm. The minimum deformation occurs at the 1st eye. Fig.24, denotes the equivalent elastic strain which is minimum at near the Centre which is equal to 3.2256e-7 unit. Fig.25, shows the maximum stress as 59.445 Mpa. The combined data of R3(1350) is given in Table.10.

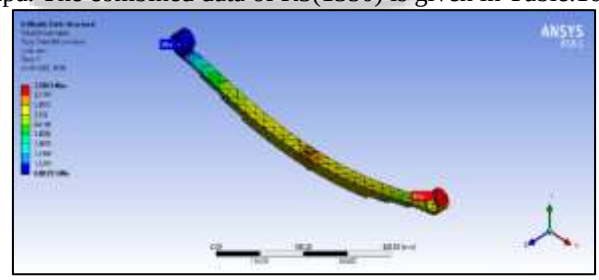

Fig. 23: Analysis image for parameters of R3(1350) Deformation.

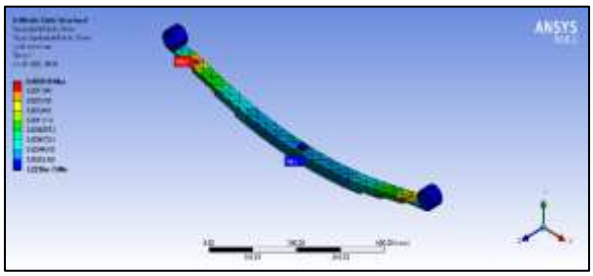

Fig. 24: Analysis image for parameters of R2(1350) Equivalent Elastic Strain.

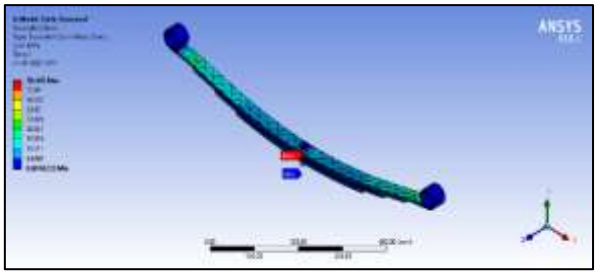

Fig. 25: Analysis image for parameters of R3(1350) Equivalent Stress.

Sr.No.	Parameter	Minimum	Maximum
1	Deformation (mm)	0.80351	7.2963
2	Equivalent elastic strain	3.2256e-7	0.002019
3	Equivalent stress (Mpa)	0.0016233	59.445

Table 10: Combined Data of R3(1350)

After applying a load of 1000N, it can be inferred from Fig.26, the maximum deformation occurred at the 2nd eye which is equal to 11.456mm. The minimum deformation occurs at the 1st eye which is equal to 1.1023 Fig.27, denotes the equivalent elastic strain which is minimum at nearby top of the 1st leaf which is equal to 2.0531e-7 unit. Fig.28, shows the maximum stress as 62.854MPa. The combined data of R1(1150) is given in Table.11.

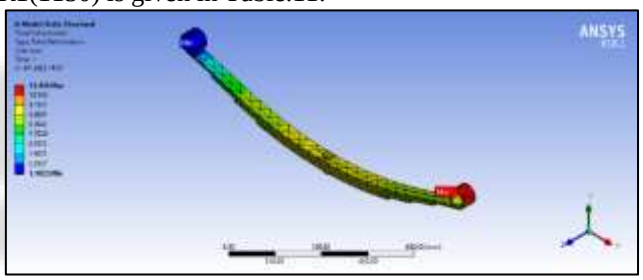

Fig. 26: Analysis image for parameters of R2(1150) Deformation.

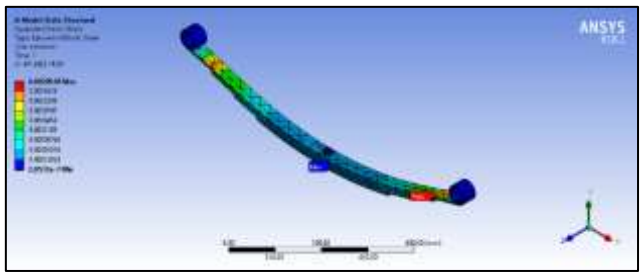

Fig. 27: Analysis image for parameters of R2(1150) Equivalent Elastic Strain.

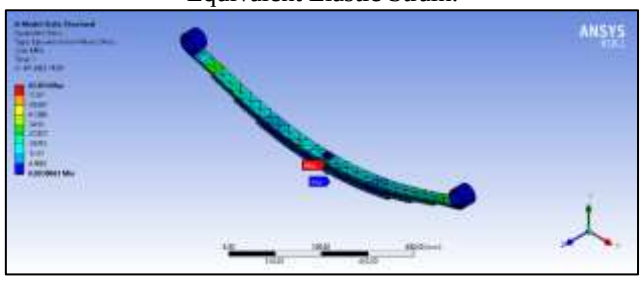

Fig. 28: Analysis image for parameters of R2(1150) Equivalent Stress.

Sr.No.	Parameter	Minimum	Maximum
1	Deformation (mm)	1.1023	11.456
2	Equivalent elastic strain	2.0531e-7	0.0029619
3	Equivalent stress (Mpa)	0.0030661	62.854

Table 11: Combined Data of R1(1150) and Load 1000N

After applying a load of 1000N, it can be inferred from Fig.29, the maximum deformation occurred at the 2nd eye which is equal to 10.294mm. The minimum deformation occurs at the 1st eye which is equal to 1.0344 Fig.30, denotes the equivalent elastic strain which is minimum at near the Centre which is equal to 3.1326e-7 unit. Fig.31, shows the maximum stress as 62.872 Mpa. The combined data of R2(1250) is given in Table.12.

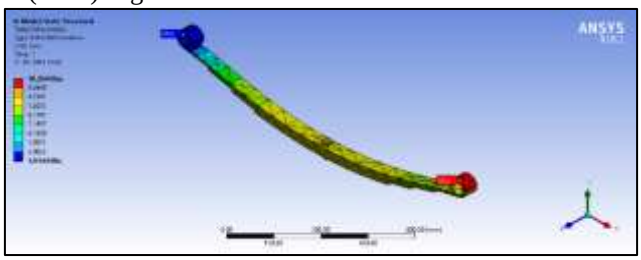

Fig. 29. Analysis image for parameters of R2(1250) Deformation.

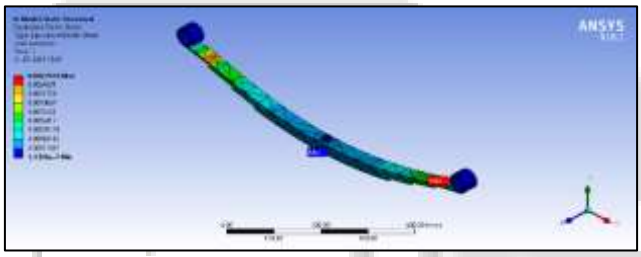

Fig. 30. Analysis image for parameters of R2(1250) Equivalent Elastic Strain.

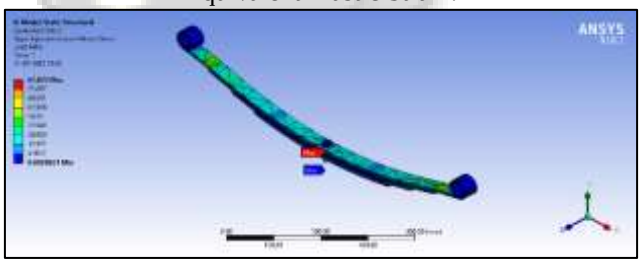

Fig. 31. Analysis image for parameters of R2(1250) Equivalent Stress.

Sr.No.	Parameter	Minimum	Maximum
1	Deformation (mm)	1.0344	10.294
2	Equivalent elastic strain	3.1326e-7	0.27935
3	Equivalent stress (Mpa)	0.0020621	62.872

Table 12: Combined Data of R1(1250) and Load 1000N

After applying a load of 1000N, it can be inferred from Fig.32, the maximum deformation occurred at the 2nd eye which is equal to 9.1204mm. The minimum deformation occurs at the 1st eye which is equal to 1.0044 Fig.33, denotes the equivalent elastic strain which is minimum at near the Centre which is equal to 4.032e-7 unit. Fig.34, shows the maximum stress as 74.306 Mpa. The combined data of R3(1350) is given in Table.13.

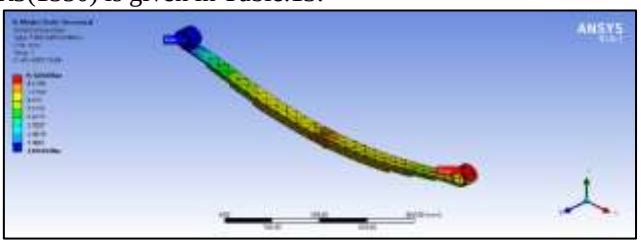

Fig. 32: Analysis image for parameters of R3(1350) Deformation.

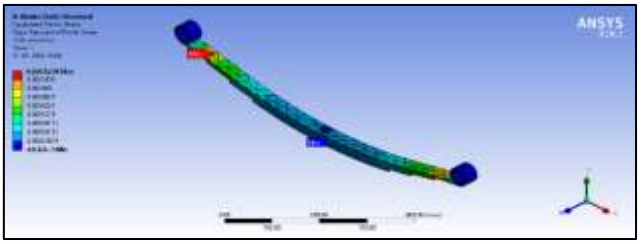

Fig. 33: Analysis image for parameters of R2(1350) Equivalent Elastic Strain.

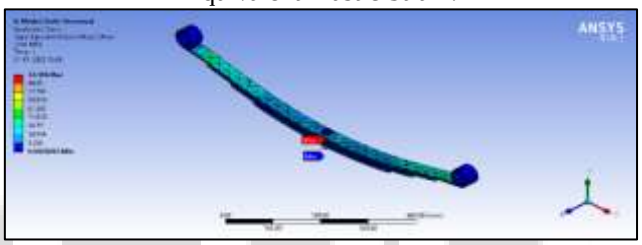

Fig. 34: Analysis image for parameters of R3(1350) Equivalent Stress.

Sr.No.	Parameter	Minimum	Maximum
1	Deformation (mm)	1.0044	9.1204
2	Equivalent elastic strain	4.032e-7	0.0025238
3	Equivalent stress (Mpa)	0.0020293	74.306

Table 13: Combined Data of R1(1350) and Load 1000N

Sr. No.	Radius	600N	800N	1000N
1	R1(1150M)	6.8735	9.1647	11.456
2	R2(1250M)	6.1762	8.235	10.294
3	R3(1350M)	5.4722	7.2963	9.1204

Table 14: Comparison of different radius (R) and Load Deformation: -

Fig. 35: Graphical representation of Deformation vs Load

Sr.No.	Radius	600N	800N	1000N
1	R1(1150M)	0.0017771	0.0023695	0.0029619
2	R2(1250M)	0.0016761	0.0022348	0.0027935
3	R3(1350M)	0.0015143	0.002019	0.0025238

Table 15: Strain

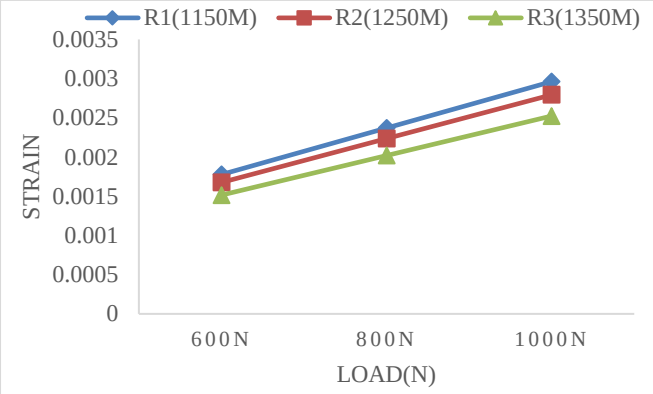

Fig. 36: Graphical representation of Strain vs Load

Sr. No.	Radius	600N	800N	1000N
1	R1(1150M)	37.712	50.283	62.854
2	R2(1250M)	37.723	50.298	62.872
3	R3(1350M)	44.584	59.445	74.306

Table 16: Stress

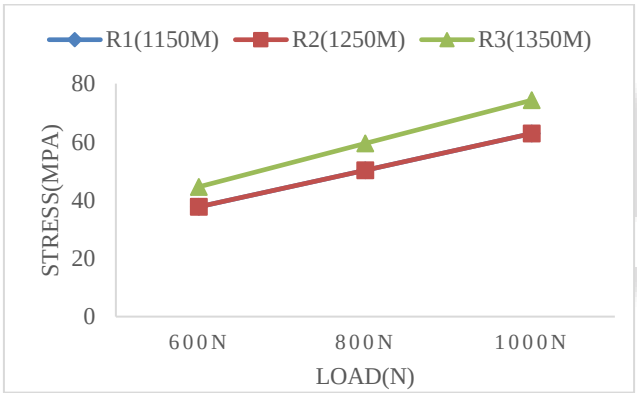

Fig. 37: Graphical representation of Stress vs Load

VIII. Conclusion

The leaf spring under static load conditions is studied and experimental results like deformation, strain, and stress are obtained with the help of ANSYS. The comparative results of all the radius are presented in Table 14,15,16 From the analysis of the different load used for producing leaf spring, the following conclusions were made

- The Radius of R3(1350) is good and it have a less deformation under the fixed support and force. Then the other two Radius.
- Radius of R3(1350) is wearing more load and is more effective
- Finally, parameters such as deformation, stress, and strain, when compared with other Radius R3(1350) have low values making it fit for leaf spring manufacturing.

IX. Declaration of Competing Interest

The authors declare that they have no known competing financial interests or personal relationships that could have appeared to influence the work reported in this paper.

X. Credit Author Statement

Abhishek Gautam : Formal analysis, Investigation, Writing - original draft preparation, Writing - review and editing; Mr. Rajesh Kumar Satankar : Resources, Supervision. All the authors read and approved the manuscript

References

[1] K. Krishnamurthy and P. Ravichandran; Sci-Hub | Modeling and structural analysis of leaf spring using composite materials | Volume 33, Part 7, 2020, Pages 4228-4232 https://doi.org/10.1016/j.matpr.2020.07.346

[2] Chala Amsalu; Sci-Hub | Mechanical characterization, and comparison of stress-induced on mono and multi-leaf spring from laminated composite material | Volume 16, December 2022, 100331https://doi.org/10.1016/j.rinma.2022.100331

[3] Birhan Alemu Tadesse; Sci-Hub | Design optimization and numerical analyses of composite leaf spring in a heavy-duty truck vehicle |Volume 62, Part 6, 2022, Pages 2814-2821 https://doi.org/10.1016/j.matpr.2022.02.367

[4] Vikas Khatkar, B.K. Behera; Sci-Hub | Textile structural composites for automotive leaf spring application | Volume 182, 1 February 2020, 107662 https://doi.org/10.1016/j.compositesb.2019.107662

[5] Anwer J. Al-Obaidi; Sci-Hub | The effect of factors on the flexural of the composite leaf spring | Volume 20, Part 4, 2020, Pages 566-571 https://doi.org/10.1016/j.matpr.2019.09.190

[6] T.G. Loganathan, K. Vinoth Kumar; Sci-Hub | Flexural and fatigue of a composite leaf spring using finite element analysis | Volume 22, Part 3, 2020, Pages 1014-1019 https://doi.org/10.1016/j.matpr.2019.11.265

[7] K. Umanath, M.K. Prabhu; Sci-Hub | Fabrication and analysis of Master leaf spring plate using carbon fibre and pineapple leaf fibre as natural composite materials |Volume 33, Part 1, 2020, Pages 183-188 https://doi.org/10.1016/j.matpr.2020.03.790

[8] Birhan Alemu Tadesse; Sci-Hub | Theoretical and finite element analysis (FEA) of coated composite leaf spring for heavy-duty truck application | Volume 62, Part 6, 2022, Pages 4283-4290 https://doi.org/10.1016/j.matpr.2022.04.782

[9] S. Seralathan; Sci-Hub | Finite element analysis of hybrid composite material based leaf spring at various load conditions | Volume 33, Part 7, 2020, Pages 3540-3548 https://doi.org/10.1016/j.matpr.2020.05.456

[10] D. Lydia Mahanthi; http://www.ijaers.com | Design and analysis of composite Leaf Spring for light Weight Vehicle Vol-4, Issue-3, Mar- 2017 ISSN: 2349-6495(P) https://dx.doi.org/10.22161/ijaers.4.3.23

[11] Abhishek Gautam; http://www.ijrpr.com/ | A Review on Modeling and Analysis of Leaf Spring Using Composite Materials in Ansys | Vol 3, no 9, pp 143-145, September 2022 https://ijrpr.com/uploads/V3ISSUE9/IJRPR6874.pdf

[12] H.A.AI-Qureshi; Sci-Hub |Automobile leaf spring. From composite materials | 118 (2001) 58-61 al-qureshi2001.pdf

[13] K.S. Ashraff Ali; Sci-Hub | Analysis of composite leaf spring using ANSYS software | Volume 37, Part 2, 2021, Pages 2346-2351 https://doi.org/10.1016/j.matpr.2020.08.068
[14] K. Ashwini; Sci-Hub | Design and Analysis of Leaf Spring using Various Composites – An Overview | vol 5, (2018) 5716–5721 ashwini2018.pdf
[15] Temesgen Batu; Sci-Hub | Multi-objective parametric optimization and composite material performance study for master leaf spring | Volume 45, Part 6, 2021, Pages 5347-5353 https://doi.org/10.1016/j.matpr.2021.01.925
[16] Fabian Becker, Christian Hopmann; Sci-Hub | Fatigue testing of GFRP materials for the application in automotive leaf springs | 19 (2019) 645–654 becker2019.pdf
[17] Ganesh R. Chavhan; Sci-Hub | Experimental analysis of E-glass fiber/epoxy composite-material leaf spring used in automotive |Volume 26, Part 2, 2020, Pages 373-377 https://doi.org/10.1016/j.matpr.2019.12.058
[18] Fei Ding, Qianlong Li, Chao Jiang; Sci-Hub | Event-triggered control for nonlinear leaf spring hydraulic actuator suspension system with valve predictive management | Volume 551, April 2021, Pages 184-204 https://doi.org/10.1016/j.ins.2020.11.036
[19] J.J. Fuentes, H.J. Aguilar; Sci-Hub | Premature fracture in automobile leaf springs | vol,16 (2009) 648–655 fuentes2009.pdf
[20] J.P. Hou; Sci-Hub | Evolution of the eye-end design of a composite leaf spring for heavy axle loads | 78 (2007) 351–358 hou2007.pdf
[21] VINKEL ARORA; IJEST| A Comparative Study of CAE and Experimental Results of Leaf Springs in Automotive Vehicles| Vol. 3 No. 9 September 2011 Pages 6856-6866 https://www.researchgate.net/publication/265262521_A_Comparative_Study_of_CAE_and_Experimental_Results_of_Leaf_Springs_in_Automotive_Vehicles?enrichId=rgreq-24e5aeecf8e7a183e8b5371cdfec914c-XXX&enrichSource=Y292ZXJQYWdlOzI2NTI2MjUyMTtBUzoyMzU4OTQzMTM1ODI1OTJAMTQzMzI1Mjk5NTQ0OQ%3D%3D&el=1_x_2&_esc=publicationCoverPdf
[22] A. Bhargav, B. Nikhil Kumar, P. Tanuj Kumar, V. Pawan; IJRPR | Design and Analysis of Leaf Spring Using Composite Materials and Prediction Using Artificial Neural Network | Vol 3, Issue 7, pp 805-817, July 2022 IJRPR5728.pdf
[23] Jenarthanan M.P, Ramesh Kumar.S, Venkatesh. G, Nishanthan.S; Sci-Hub | Analysis of leaf spring using Carbon / Glass Epoxy and EN45 using ANSYS: A comparison | vol 5,(2018) 14512–14519 jenarthanan2018 (1).pdf
[24] L.B. Chua; Sci-Hub | Fatigue life prediction of parabolic leaf spring under various road conditions | Volume 46, November 2014, Pages 92-103 https://doi.org/10.1016/j.engfailanal.2014.07.020
[25] Krishan Kumar, M.L. Aggarwal; Sci-Hub | Optimization of Various Design Parameters for EN45A Flat Leaf Spring | vol 4,(2017) 1829–1836 http://www.materialstoday.com/proceedings
[26] Jun Ke, Zhen-yu Wu; Sci-Hub | A review on material selection, design method and performance investigation of composite leaf springs | Volume 226, 15 October 2019, 111277 https://doi.org/10.1016/j.compstruct.2019.111277
[27] Chirag D. Bhatt, Mukesh Nadarajan; Sci-Hub | Leaf spring model for heavy load vehicle using solid works and ANSYS analysis | Volume 33, Part 7, 2020, Pages 4764-4770 https://doi.org/10.1016/j.matpr.2020.08.360
[28] Pradip Kumar; Sci-Hub | Analysis and optimization of mono parabolic leaf spring material using ANSYS | Volume 33, Part 8, 2020, Pages 5757-5764 https://doi.org/10.1016/j.matpr.2020.06.605
[29] I. Rajendran; Sci-Hub | Optimal design. Of a composite leaf spring using genetic algorithms | 79 (2001) 1121-1129 leaf5.pdf
[30] Bathuka Mallesh, Balaji Gupta, S. Kranthi Kumar Sci-Hub | Modeling and analysis of leaf spring with a different type of materials | Volume 45, Part 2, 2021, Pages 1945-1949 https://doi.org/10.1016/j.matpr.2020.09.223
[31] R. Naresh; Sci-Hub | Static and Transient Response of a Leaf Spring with EPDM Rubber Sandwiched Between Steel Leaves | 22 (2020) 3250–3260 http://www.materialstoday.com/proceedings
[32] Ashish Kumar Shrivastava, Rohit Pandey, Hardik B. Ramani, Shiv Nandan Chourasia; Sci-Hub | Modal analysis of polymer composite based leaf spring by additive layer manufacturing using FEA method | Volume 47, Part 19, 2021, Pages 7091-7094 https://doi.org/10.1016/j.matpr.2021.06.183
[33] Harmeet Singh; Sci-Hub | Characterization and Investigation of Mechanical Properties of Composite Materials used for Leaf Spring | 5 (2018) 5857–5863 http://www.materialstoday.com/proceedings
[34] Pulkit Solanki; Sci-Hub | Design and computational Analysis of Semi-Elliptical and Parabolic Leaf Spring | 5 (2018) 19441–19455 http://www.materialstoday.com/proceedings
[35] Hiroyuki Sugiyama; Sci-Hub | Development of nonlinear elastic leaf spring model for multibody vehicle systems | 195 (2006) 6925–69 sugiyama2006.pdf
[36] Nishant Varma, Ravi Ahuja, T. Vijayakumar; Sci-Hub | Design and analysis of composite mono leaf spring for passenger cars | Volume 46, Part 17, 2021, Pages 7090-7098 https://doi.org/10.1016/j.matpr.2020.10.073
[37] A.P. Venkatesh, S. Padmanabhan, C. Allen Rufus, H. Mohammed Lukmaan, A.R. Abdul Rahman; Sci-Hub | Exploration of fatigue and modal analysis on mono leaf suspension made by natural composite materials | Volume 47, Part 14, 2021, Pages 4262-4267 https://doi.org/10.1016/j.matpr.2021.04.568

